THE GEOLOGICAL SOCIETY OF AMERICA

Technical Note

Kinematics of a Translational/Rotational Landslide, Central Andes, Northwestern Argentina

LILIANA DEL VALLE ABASCAL

U.N. Salta-CADIC, Av. B. Houssay 200, Ushuaia, 9410 Tierra del Fuego, Argentina

GUSTAVO GONZÁLEZ BONORINO

CADIC-CONICET, Av. B. Houssay 200, Ushuaia, 9410 Tierra del Fuego, Argentina

Key Terms: ***Landslide, Argentina, Andes, Landslide Hazard, Risk***

INTRODUCTION

The eastern foothills of the Central Andes, known as the Subandean Ranges, in Peru, Bolivia, and northwestern Argentina, are characterized by heavy rainfall, weakly cemented substrate rocks, thick regoliths, and bedding planes parallel to mountain slopes, features that create serious landslide hazards (Multinational Andean Project: Geoscience for Andean Communities, http://www.pma-map.com). A moderately sized landslide (the Termas Hill landslide) occurred in August 2003 on a slope of the Andean foothills in northwestern Argentina (Figure 1). The slide disrupted regolith and rock, leaving a steep-walled scarp and severing a 130-m-long segment of forest road. The sliding block travelled downslope a few tens of meters, undergoing fragmentation and torsion. On the basis of a topographic survey and structural evidence, this article discusses the geometry and kinematics of the Termas Hill landslide.

GEOGRAPHIC AND GEOLOGIC SETTING

The Subandean Ranges in northwestern Argentina (22–26°S; Figure 1A and B) have a humid subtropical climate with annual precipitation of 700–1,200 mm and an average air temperature of 20°C. The climate is mild with a dry winter season. Rainfall is concentrated in the austral summer months and is of the monsoonal type (Figure 1D). The Subandean Ranges are aligned in a north-south direction, with mountain tops commonly below 2,500 m above sea level (a.s.l.) Vegetation is lush, of mountain forest type, with deciduous and evergreen tree species up to 25 m tall. The biologically diverse ecosystem is regionally known as ''yunga'', or ''warm valley'', in Quechua aboriginal language.

The Subandean Ranges are part of the Andean fold-and-thrust belt (González-Bonorino et al., 2001). Individual ranges are underlain by anticlinal folds, which may be thrusted. In the study area, the fold-and-thrust belt involves a 5–7 km-thick sedimentary succession, Paleozoic to Quaternary in age, which rests unconformably on a Proterozoic, low-grade metasedimentary basement. Upper Tertiary to lower Quaternary deposits constitute a wedge of continental foreland basin deposits shed from the rising Andes. Structural deformation in the Subandean Ranges largely is Quaternary in age, which is manifest in the common occurrence of wind and water gaps carved by antecedent river courses. Subandean outcrops mostly consist of sandy continental deposits showing weak cementation and thus are prone to erosion by surface flows and gravitational collapse. Abundant rainfall and steep slopes have given rise to thick regoliths composed of colluvial deposits capped by acidic, poorly developed, shallow soils derived from sedimentary rocks (Nadir and Chafatinos, 1995).

The area of specific interest to our study lies in the southernmost portion of the Subandean Ranges, in the province of Salta. In this area, a major anticline (Termas Hill anticline) in upper Tertiary sedimentary rocks plunges northward under recent alluvial deposits. The anticline is cut by east-verging thrusts and reverse antithetic faults (Figure 1C). The northern tip of the anticline underlies the Termas Hill, and is traversed by a wind gap presently occupied by provincial road 34 (Figure 1C). The Termas Hill landslide occurred on the western limb of the Termas Hill anticline about 1 km south of the wind gap (Figure 1C). Thermal waters seep through fractures near the base of Termas Hill, at about 880 m a.s.l. (Moreno et al., 1975; Seggiaro et al., 1997), and a hotel dating from the early 20th century was built

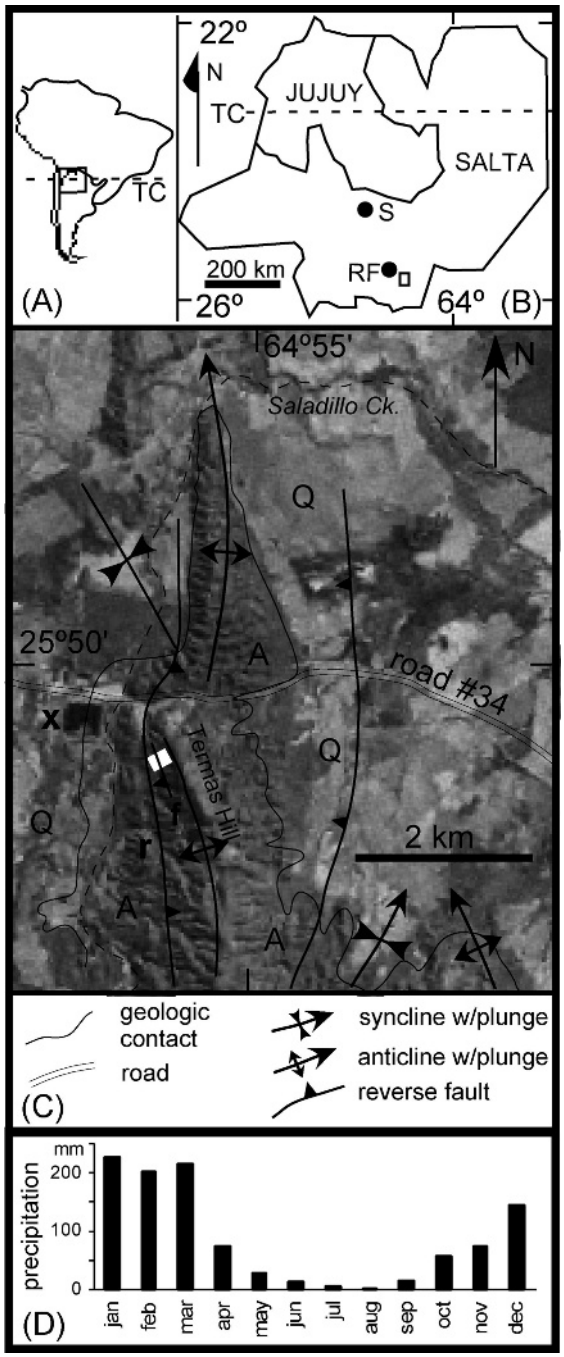

Figure 1. Location maps. (A) South America with Argentina outlined and square representing inset B (TC = Tropic of Capricorn). (B) Salta Province (S = Salta City; RF = Rosario de la Frontera; TC = Tropic of Capricorn; open rectangle shows location of map in inset C). (C) Simplified geologic map overlaid on a Thematic Mapper satellite image (white rectangle represents area of landslide; x = campsite adjoining large pond; r = topographic ridge; f = reverse fault affecting Termas Hill landslide; Q = Quaternary deposits; A = Anta Formation, geology taken from Seggiaro and others, 1997). (D) Average rainfall between 2000 and 2005, inclusive; meteorological station located 30 km north from landslide site, in similar geomorphic and climatic situation.

around these springs. A service road connects the hotel with a communications antenna, passing through the area of the landslide with a bearing of 330 degrees. At the foot of the slope, Saladillo Creek flows northward and around the nose of the anticline. The floor of the creek lies 1–2 m below the surface of an alluvial plain open to the west and northwest (Figure 1C).

The landslide site (25°50′40″S, 64°55′49″W) is underlain by strata of the upper Tertiary Anta Formation, an alluvial/lacustrine sedimentary unit at the base of the foreland basin succession. The Anta Formation consists of thick-bedded, coarse-grained sandstone and thin intercalated layers of greenish mudstone dipping 35°W. Unconformably overlying these strata is a thick (2–8 m thick) regolith of blocky sandstone debris in a slightly indurated matrix (GM in the Unified Soil Classification System; ASTM, 2000) and lenses of mudstone breccia derived from underlying Anta Formation strata, capped by an immature soil profile about 0.5–1-m thick. Locally, the bedrock and the regolith are slightly altered because of percolation of thermal waters (Abascal et al., 2006). Bush and tree roots are dense in the uppermost 0.5 m and generally decrease to nil with depth within the regolith; however, some long tree roots extend several meters into the ground. Root development is mostly unaffected by the hard rock substrate and qualifies as a type D soil-root system in the nomenclature scheme of Tsukamoto and Kusakabe (1984). A reverse fault cuts the western flank of the Termas Hill anticline intersecting the landslide scarp (f in Figure 1C). A secondary, very young reverse fault (not shown), approximately parallel to the road and dipping 60°W, brings up strata of the Anta Formation against regolith. The western flank of Termas Hill shows a rock ledge at about 900 m a.s.l. upfaulted by an antithetic reverse fault. The ledge develops northward into a topographic ridge separated from the main mountain body by an intervening valley (Figures 1C, 2, and 3A).

THE TERMAS HILL LANDSLIDE

The Termas Hill landslide occurred in August 2003, during the austral winter and well into the dry season. Rainfall records for August 2003 indicate only 5 mm of precipitation concentrated on August 5th. The area neighboring the site of the slide is sparsely populated and the day on which the slide took place could not be precisely constrained. The landslide caused material damage to the service road and no human casualties. The provincial newspaper El Tribuno invited a geologist to conduct an informal site assessment. The conclusions from that expeditive

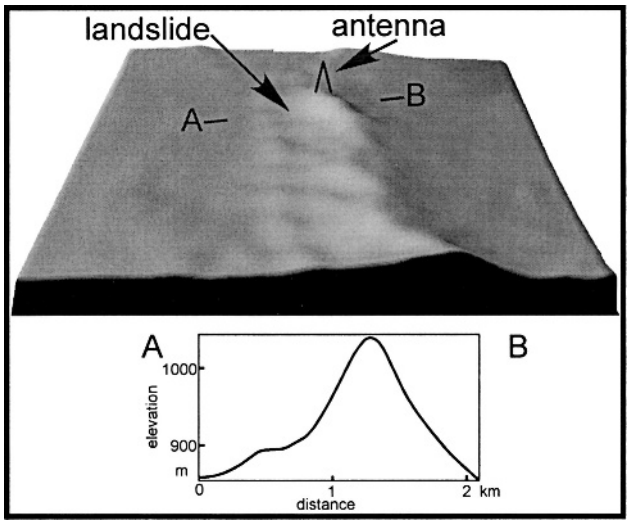

Figure 2. Digital elevation model (DEM) of the Termas Hill area and elevation profile across the site of the slide, showing the upfaulted rock ledge. This ledge partly protects base-of-slope areas from landslides generated on the western flank of Termas Hill. DEM obtained from Shuttle Radar Topographic Mission images processed with 3DEM software of the U.S. Geological Survey. View northward. The position of the communications antenna is indicated.

report published by the newspaper were alarming: the Termas Hill was toppling down in successive slides, and damming of Saladillo Creek and subsequent disastrous rupture of the dam was foreseeable. In panic, a few local residents put their houses up for sale.

Given the impending summer holidays and rainy season, municipal authorities of Rosario de la Frontera, a town of 15,000 inhabitants located 6 km northwest from the landslide site, were highly concerned over a reactivation of the Termas Hill and other potential slides. Particular focus was placed on the nearby hotel and a campsite located on the left margin of Saladillo Creek (X in Figure 1C), downstream from the site that was predicted to be flooded by landslide damming of the creek. Consequently, these authorities requested that the provincial government organize a formal inspection of the site. An interinstitutional party of three geoscientists visited the site on September 2003 and generally supported, in more moderate terms, the previous conclusions regarding risk. Seeking confirmation for these reports, provincial civil defense authorities contacted Salta University for professional counsel. The present authors inspected the site on February 2004. Our conclusions differed substantially from previous assessments regarding the mechanics of the slide and the hazard it posed. Subsequent inspections in July 2004, February 2005, and February 2006 supported those conclusions.

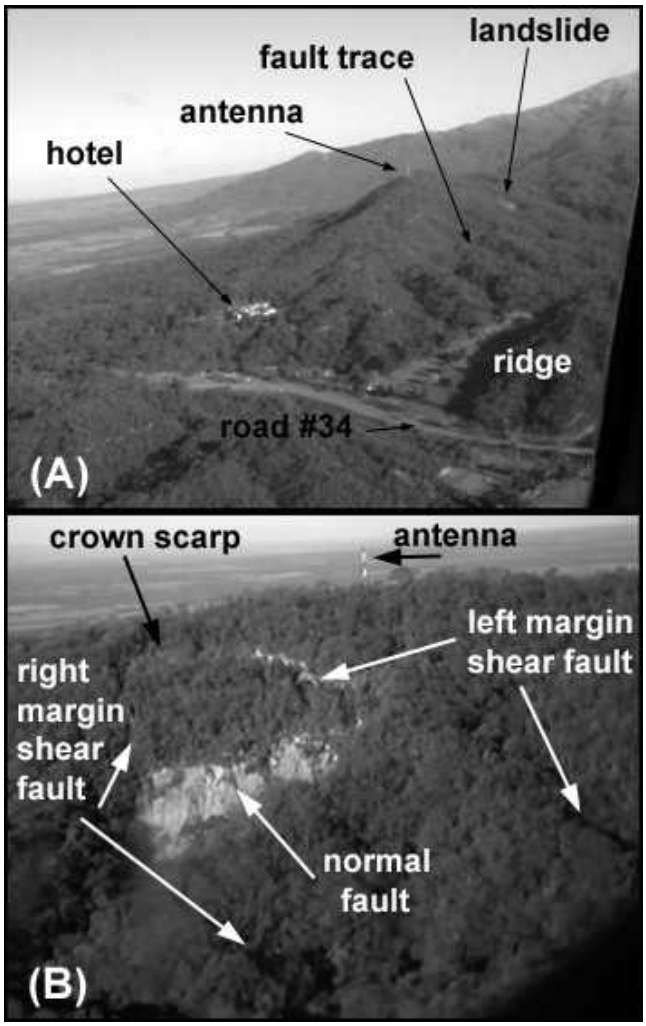

Figure 3. Aerial views. (A) View to the south-southeast showing the landslide site on the western flank of Termas Hill. Road 34 follows wind gap. (S = Saladillo Creek partly hidden by airplane wing). (B) View east-southeast showing main structural features of the Termas Hill landslide. Note the trace of shear faults in vegetated slope. Photographs courtesy of J. G. Viramonte.

Description of the landslide

The Termas Hill landslide involved the displacement in the downslope direction of a rectangular area of mountain slope approximately 130-m wide and 300-m long. The crown of the slide lies at 1,040 m a.s.l., 10 m below the local ridge crest. The toe lies at about 900 m a.s.l., at the level of the faulted rock ledge. The base of the local slope, and the course of Saladillo Creek, is at about 850 m a.s.l. The crown scarp is up to 8 m in height (Figure 4A) and locally preserves the original surface of rupture dipping 60–80° downslope. Laterally, the slide is bounded by two parallel shear faults 130 m apart. The topographically higher reaches of the shear fault planes dip 65–70° into the slide. In plan view, the crown scarp is slightly

Figure 4. (A) Crown scarp. Note the shallow root zone. In the foreground is rotated slump left behind by the slide. (B) Scarp of the right-margin shear fault curves into the crown scarp in the background.

concave downslope and merges smoothly with the scarps formed by the lateral shear faults (Figure 4B). The lateral scarps severed the service road almost at right angles. Between the crown scarp and the undisturbed part of the road, the lateral scarps cut entirely into regolith; from that point on they cut through upfaulted strata of the Anta Formation for at least 30 m downslope (Figure 5C). Further downslope, the scarp is not apparent and the traces of the shear faults show as a discontinuity in the vegetation (Figure 3B). The basal slip surface is located at the top of a layer of greenish mudstone of the Anta Formation, which dips 35°W. The mudstones were highly plastic at the time of our first inspection in February 2004, during the rainy season, and less so in subsequent visits to the site.

At the time of our first inspection, both lateral scarp surfaces showed well developed striations (Figure 5B); these were eroded away in succeeding months. Striations plunged downslope, on average, 45° on the right-margin (looking downslope) scarp surface and 32° on the left-margin scarp surface. In addition to the striae, the right-margin scarp surface showed pluck marks indicating displacement obliquely up the scarp of the landslide body (Figure 5A).

The offset road segment, presently located 30 m downslope from its original position, consists of a central 90-m-long straight segment bounded at each end by shear zones associated with the lateral faults. A narrow (about 5-m wide) shear zone adjoins the right margin scarp (Figure 6B), whereas toward the left margin closely spaced *en echelon* faults deformed the road into an arcuate trace (Figure 6A). The displaced road segment is traversed perpendicularly by tension cracks measuring up to 4 m in length and 3 m in depth (Figures 5C and 7A). In addition, a few compression ridges developed perpendicular to the road. The largest compressive ridge adjoins the right margin scarp, rising to 0.4 m above the surrounding road level (Figures 5C and 7A). A subdued ridge is present in the central reach of the displaced road segment.

The head of the slide includes the displaced road segment. The depletion zone measures about 30 m in downslope width and is largely covered by debris (Figure 7B). The head of the slide rises 3–5 m above the floor of the adjoining depletion zone, a situation that has led to ponding of rainwater and deposition of horizontal laminae of mud and fine sand over an elongate area parallel to the main scarp and about 60-m long and 3-m wide. An isolated ridge of displaced material carrying in situ vegetation is located at the northeastern corner of the slide area; the ridge crest rises 3.5 m above the level of the pond (Figure 7A). A subordinate volume of detritus occurs as talus and slumps along the foot of the main and lateral scarps. A comparison of photographs taken by other parties in October 2003 and by us in February 2004 suggests that most of the detritus accumulated during and shortly after the slide event. Approximately 150 m

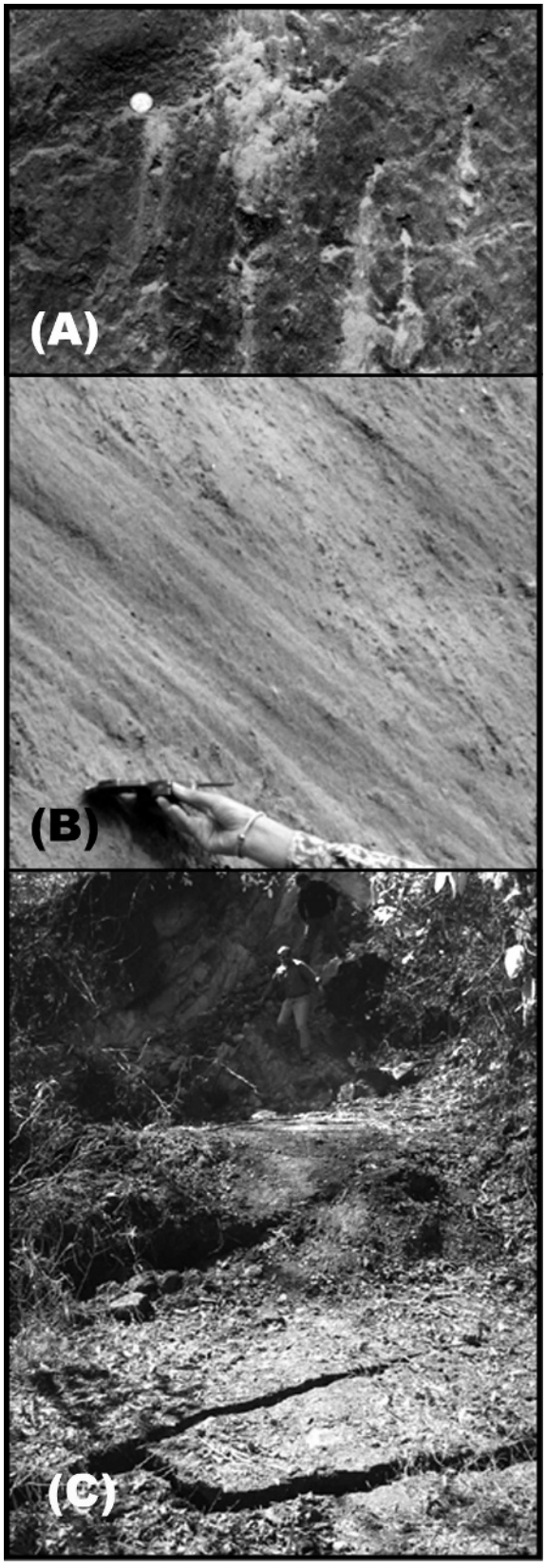

Figure 5. (A) Pluck marks slightly inclined downslope and downstepping up the scarp indicate initial upward movement of the slide block. Coin on pluck step measures 1.5 cm in diameter.

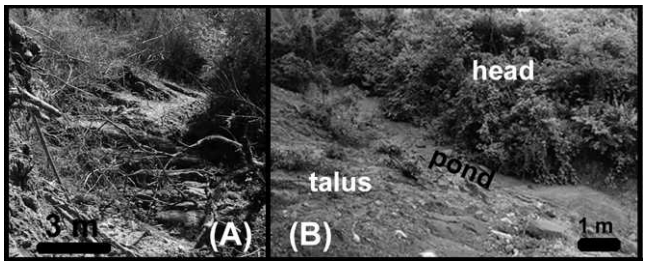

Figure 6. (A) The sheared and segmented southern end of the service road. Note *en échelon* pattern of faults. Scale valid in middle ground. (B) The vegetated head of the slide has dammed running water, giving rise to an ephemeral pond; vegetation traveled with the slide. Talus from the crown scarp can be seen in the foreground. View oblique downslope.

downslope from the crown scarp, a normal fault dipping 60°W severed the displaced material into two slide units of similar area. At the normal fault, the downthrown block rotated into the Termas Hill. The trace of the lateral faults bounding the lower slide unit can be recognized from the disrupted pattern of the vegetation, but the faults themselves are not exposed.

The volume of the Termas Hill slide is uncertain because its thickness is unknown downslope from the normal fault. Assuming a uniform thickness of 8 m yields an estimate of 310,000 m^3 and implies a shear stress of roughly 130 kPa. Tree surcharge for the Termas Hill slide is estimated at 1 kPa and is relatively insignificant. The root network can contribute significantly to the strength of a soil (Hammond et al., 1992). The Termas Hill slide severed roots up to 3 cm in diameter, and others several meters long were pulled out from the lateral walls. For thick regolith, however, the root factor is insignificant in the total force system (Hammond et al., 1992). Soil strength caused by mineral cohesion is low for colluvium, on the order of a few kilopascals. The plastic mudstones underlying the basal fault must have offered little resistance to sliding. Most of the resistance should have originated in the upfaulted strata of the Anta Formation. The tensile strength of intact sandstone rates at about 2–6 MPa (Sklar and Dietrich, 2001), but joints and weathering can decrease this value to much less than half (Selby, 1980).

←

(B) Striations on the right-margin scarp plunge 35° downslope. (C) View toward the northern lateral fault plane exposing strata of the Anta Formation in the background and part of the displaced service road in the foreground. Note the tension cracks near the bottom of the photograph and he compression ridge in the middleground. Person for scale. Photograph courtesy of J. G. Viramonte.

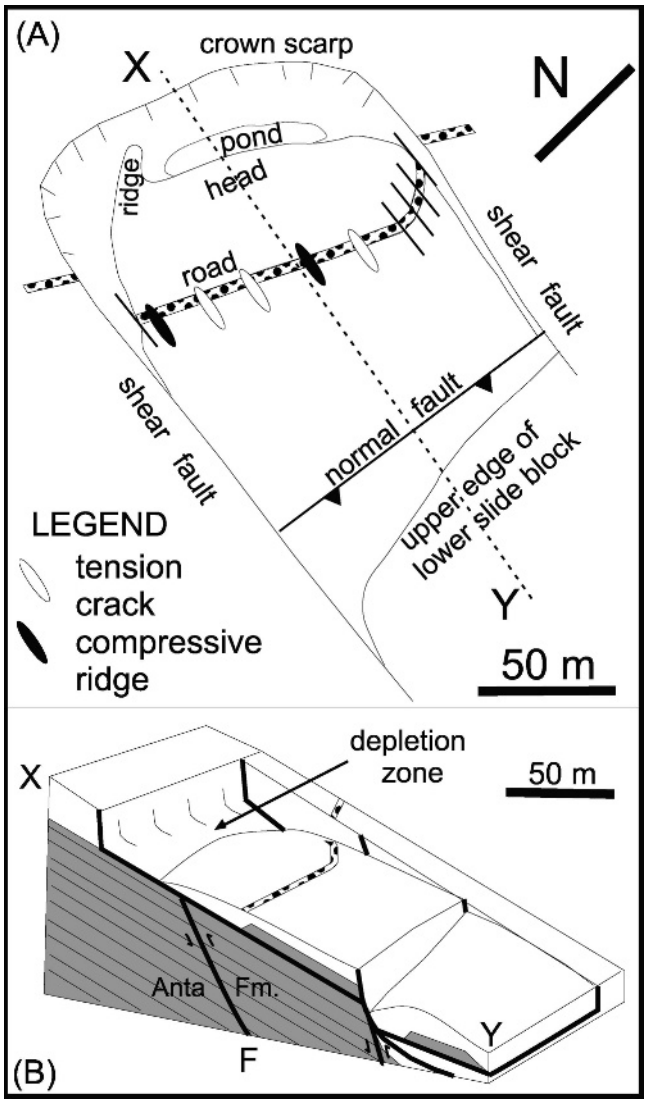

Figure 7. Schematic of the Termas Hill landslide. (A) Plan view. (B) Block diagram along dashed line XY in A (regolith in white; Anta Formation in light gray). The subsurface structure in the right half of diagram is speculative. Note the main slip surface cut by a subsequent normal listric fault. See text for description.

DISCUSSION OF SLIDE KINEMATICS

The minimum runout length for the slide is 30 m, measured from the crown scarp to the head of the slide. There are no witnesses to establish whether the slide detached and moved to its present position in one rapid event or involved tensional cracking at the crown fault followed by slow creep. The first alternative is considered more likely because a persistent open crack would be partially filled by a wedge of mineral and vegetal debris washed from the crown, for which no evidence exists. Circumstantial evidence in support of rapid movement is provided by several large trees toppled in a downslope direction, as would be expected following sudden arrest of a fast-moving slide.

Striations on the left-margin scarp surface plunge parallel to the dip of the greenish mudstone layers, indicating translational movement of the slide. Striations on the right-margin scarp surface plunge at an angle 5–10° higher than in the Anta Formation and are spatially associated with pluck marks that indicate reverse offset at this shear fault. It is tentatively suggested that plucking occurred first because of upward displacement of the slide block against the right-hand wall and that the striations developed immediately after as the slide settled downslope from a topographic position slightly higher than that of the left slide margin.

Compressive ridges adjoining marginal shear faults have been observed in other landslides (e.g., Baum and Fleming, 1996). In the Termas Hill slide, the prominent ridge close to the right-margin fault may have developed under transpression. The subdued ridge in the central sectors of the displaced road segment, away from the lateral faults, is attributed to compression as the slide adapted to an underlying topographic depression, probably a valley head. The tension cracks, in turn, probably reflect torsion about vertical axes, related to drag on the lateral faults.

Thick regolith resting upon 35°-dipping strata, an inclination similar to the angle of repose for colluvium, is intrinsically unstable. Instability would have been enhanced by the substrate of plastic mudstone. Furthermore, the crown of the slide is very close to the hinge of the Termas Hill anticline. Badger (2002) pointed out the importance to landsliding of fractures associated with anticlinal folding. One set of fractures tends to develop perpendicular to bedding and to the fold axis (Price and Cosgrove, 1990). Badger (2002) judged this set of fractures to be kinematically irrelevant in the cases he studied. In the case of the Termas Hill slide, however, such a set of fractures may have been at the origin of the sharp and rectilinear lateral faults. Undoubtedly, weathering and joints weakened the Anta Formation sandstone beds, facilitating cutoff by the basal fault.

The slide block is cut in two by the normal fault at half length (Figure 7A). Inward rotation near the fault suggests the action of a listric normal fault. It is postulated that the translational displacement occurred first, affecting slide blocks on both sides of the normal fault and that the rotational displacement occurred immediately, or shortly, after (Figure 7B). Normal faulting probably reactivated the reverse fault upholding the rock ledge and may have been favored by a thickening of the colluvium in the lower slope of Termas Hill. The position of the toe of the slide may have been governed by the rock ledge flanking Termas Hill (Figure 2).

The trigger for the Termas Hill landslide remains in doubt. Heavy rainfall and earthquakes can be ruled out, given that the Termas Hill slide occurred in the driest part of the year (cf. Figure 1C) and that no significant earthquakes were reported from that area in July–August. A surge of thermal water may have occurred, wetting the plastic clay in the Anta Formation. Alternatively, considering that throughout the dry season the clay retains some plasticity, detachment may be attributed to creep leading to fracture and fast displacement thereafter.

CONCLUSIONS AND RISK ASSESSMENT

Photographs taken one month after the slide event by other parties, when compared with our observations, served to show that the bulk of the slide did not undergo noticeable displacement in the following 17 months, which included two rainy seasons. Two factors may have contributed to locking the slide after the initial surge: one is termination of the plastic shale bed at fault F (Figure 7); the other is sandstone-sandstone friction along the sliding surface, downslope from fault F. Retreat of the main scarp through mass wasting has contributed a significant amount of loose material, most of which remained stored in the talus at the foot of the main scarp and in the pond upslope from the head of the slide. Saladillo Creek did not show any noticeable change in color that could be attributed to input of detritus from the slide scar. Risk derived from possible damming of Saladillo Creek by a reactivated Termas Hill slide, or other slide, is low because of the small hydraulic radius of the creek and the open expanse of alluvial plain onto which excess water would drain.

From a wider viewpoint, the hazard of further slide events along the western flank of Termas Hill remains high because of structural and stratigraphic conditions similar to those at the site of the Termas Hill slide. This issue was analyzed with the Level I Stability Analysis (LISA) computer model for relative landslide hazard evaluation (Hammond et al., 1992). LISA estimates a probability of failure from iterated Monte Carlo simulations of a safety factor. Results yielded a probability of failure of about 0.2, a value that rates as high landslide hazard (Hammond et al., 1992). The vulnerability, however, is low because of sparse population and little infrastructure in areas within probable reach of a landslide. In addition, the rock ledge in the lower slope would slow down and act to disaggregate a coherent slide. In the future, however, landslide risk should be better qualified through acquisition of geotechnical data and numerical slope-stability analysis.

Initial risk assessments drew on generalized prejudice that the area is prone to landslide events and were not based on specific study of the Termas Hill slide. The alarming reports, however, motivated provincial and municipal authorities to act responsibly and seek professional counsel. Once the specific hazard had largely deactivated, authorities declined to implement even the modest safety measures recommended by us.

ACKNOWLEDGMENTS

We are grateful to Dr. J. Viramonte (Universidad Nacional de Salta) for providing several photographs. We thank the support given to us by the municipality of Rosario de la Frontera. Critical comments by reviewers for *Environmental and Engineering Geoscience*: William Cole (Geoinsite, Inc.), Robert L. Schuster (U.S. Geological Survey) and an anonymous colleague, greatly helped to improve the manuscript.

REFERENCES

Abascal, L. del V.; González Bonorino, G.; and Viramonte, J. G., 2006, Influencia de la topografía y alteracion hidrotermal en la deformación interna de un deslizamiento por traslación, Sierras Subandinas, Salta, Argentina, in *Actas, III Congreso Argentino de Cuaternario y Geomorfología*, Universidad Córdoba, Vol. 1, pp. 487–493.

ASTM, 2000, *Standard Classification of Soils for Engineering Purposes (Unified Soil Classification System)*: D2487-00 ASTM International, 12 p.

Badger, T. C., 2002, Fracturing within anticlines and its kinematic control on slope stability: *Environmental and Engineering Geoscience*, Vol. 8, No. 1, pp. 19–33.

Baum, R. L. and Fleming, R. W., 1996, Kinematic studies of the Slumgullion Landslide, Hinsdale County, Colorado. In Varnes, D. J. and Savage, W. Z. (Editors), *The Slumgullion Earth Flow: A Large-Scale Natural Laboratory*, Chapter 2: U.S. Geological Survey Bulletin 2130, pp. 9–12

González-Bonorino, G.; Kraemer, P.; and Re, G., 2001, Andean Cenozoic foreland basins: a review: *Journal South American Earth Sciences*, Vol. 14, pp. 651–654.

Hammond, C.; Hall, D.; Miller, S.; and Swetik, P., 1992, *Level I Stability Analysis (LISA) documentation for version 2.0*: GTR INT-285, Intermountain Research Station, USDA Forest Service, 190 p.

Moreno, E. C. H.; Viramonte, J. G.; and Arias, J. E., 1975, Geología del área termal de Rosario de la Frontera y sus posibilidades geotérmicas. In *Actas, II Congreso Iberoamericano de Geología Económica,* Vol. 2: pp. 543–560.

Nadir, A. and Chafatinos, T., 1995, *Los suelos del N.O.A. Salta, Argentina*: Cámara del Tabaco, Salta, 220 p.

Price, N. J. and Cosgrove, J. W., 1990, *Analysis of Geologic Structures*: Cambridge University Press, Cambridge, U.K., 502 p.

Seggiaro, R.; Aguilera, N.; Ferretti, J.; and Gallardo, E., 1997, Estructura del area geotérmica de Rosario de la

Frontera, Salta, Argentina. In *Actas, 8° Congreso Geológico Chileno,* Universidad Católica del Norte Antofagasta, Vol. 1: pp. 390–393.

Selby, M. J., 1980, A rock mass strength classification for geomorphologic purposes with tests from Antarctica and New Zealand: *Zeitschrift für Geomorphologie*, Vol. 24, pp. 31–51.

Sklar, L. S. and Dietrich, W. E., 2001, Sediment and rock strength controls on river incision: *Geology*, Vol. 29, No. 12, pp. 1087–1090.

Tsukamoto, Y. and Kusakabe, O., 1984, Vegetative influences on debris slide occurrences on steep slopes in Japan: *Honolulu, HI*, Environment and Policy Institute, East-West Center, pp. 63–72.